MOLECULAR CHARACTERISTICS

OF PORT WINE STAINS

by

Karol Lynne Wright

A thesis submitted to the faculty of
The University of Utah
in partial fulfillment of the requirements for the degree of

Master of Science

in

Laboratory Medicine and Biomedical Science

Department of Pathology

The University of Utah

May 2015

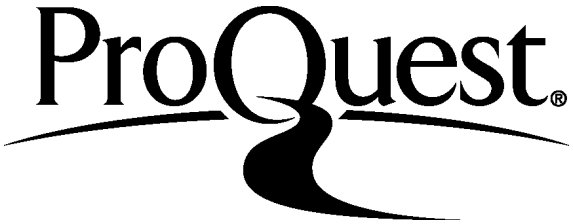

The University of Utah Graduate School

STATEMENT OF THESIS APPROVAL

The thesis of **Karol Lynne Wright**

has been approved by the following supervisory committee members:

Pinar Bayrak-Toydemir	, Chair	**03/23/2015** Date Approved
David A. Stevenson	, Member	**03/25/2015** Date Approved
Whitney L. Wooderchak-Donahue	, Member	**03/23/2015** Date Approved

and by **Peter E. Jensen** , Chair/Dean of

the Department/College/School of **Pathology**

and by David B. Kieda, Dean of The Graduate School.

ABSTRACT

Port wine stains are capillary malformations that are typically located in the dermis of the head and neck. They affect 0.3% of the population. Current theories suggest that port wine stains are caused by somatic mutations that disrupt vascular development. I hypothesize that port wine stains are multifactorial and understanding their genetic determinants could provide insight into novel treatments. This study used a custom next generation sequencing panel and digital polymerase chain reaction to investigate genetic variants in 12 isolated port wine stain cases (i.e., individuals with port wine stain alone). Novel variants were identified in *GNAQ, SOX10,* and *RASA1*. The previously identified *GNAQ* c.548G>A, p.Arg183Gln mutation was confirmed in 9 of 12 cases with an allele frequency ranging from 1.73 to 7.42%. The custom next generation sequencing panel allowed for detection of low level mosaicism found in 10 of 12 isolated port wine stain cases. A novel *GNAQ* c.547C>G, p.Arg183Gly mutation was identified in one case. Digital polymerase chain reaction confirmed novel variants detected by next generation sequencing. The results from both methods were highly concordant providing an effective way to detect low level mosaicism in port wine stains. Importantly, the identification of novel genetic mutations in port wine stains may facilitate the development of novel treatments.

TABLE OF CONTENTS

LIST OF TABLES

LIST OF FIGURES

ACKNOWLEDGEMENTS

To my Supervisory Committee:

Pinar Bayrak-Toydemir, M.D., Ph.D.

David Stevenson, M.D.

Whitney Wooderchak-Donahue, Ph.D.

I would like to thank all of you for giving me this opportunity and assisting me with this project. This has been a great learning experience that was made better with your input and guidance. I would especially like to thank Whitney for her assistance and patience throughout the entire project. I would also like to thank Alice Frigerio for here assistance with the data analysis and the individuals who assisted with running samples on the HiSeq instruments.

INTRODUCTION

Literature Review

Vascular anomalies are a group of disorders represented by abnormal development of blood vessels. These disorders are classified into either vascular tumors or vascular malformations according to the International Society for the Study of Vascular Anomalies (ISSVA) guidelines (Lowe, Marchant, Rivard, & Scherbel, 2012). Vascular malformations are further divided depending on the type of vessel affected. Port wine stains (PWS, OMIM 163000) are abnormal development of the capillary vessels, also called capillary malformation (CM).

PWS are present at birth as a pink, well-marked patch that will gradually thicken and darken over time. They are more common on the face and neck, but do occur in other locations. Histology describes PWS as dilated capillary-like vessels with normal endothelial cells and decreased neuronal markers (Smoller & Rosen, 1986). Most cases of PWS are isolated, but recently Rubin et al. (2015) has reported familial cases. Port wine stains are present in 3 of 1,000 individuals (Jacobs & Walton, 1976).

The etiology of PWS is unclear, but one theory suggests that they are caused by a somatic mutation that disrupts early vascular development (Happle, 1987). Shirley et al. (2013) was able to confirm this theory with the identification of a somatic mutation in *GNAQ* (c.548G>A, p.Arg183Gln) in 12 of 13 isolated PWS cases. *GNAQ* is a guanine nucleotide binding protein that regulates signals between the G-protein-coupled receptors

and the downstream effectors (Shirley et al., 2013).

Another theory I suggest is that port wine stains are caused by a somatic event that occurred during neural crest cell development and specialization. *SOX10* is a transcription factor that is necessary for specific cell fates during neural crest development. *PAX3* is another transcription factor that is crucial for neural crest cell development. Mutations in *SOX10* and *PAX3* have been reported in cases of Waardenburg syndrome, which results in sensorineural deafness and pigmentation defects (Bondurand et al., 2000).

Mutations in *RASA1* have been identified in cases of capillary malformation-arteriovenous malformation (CM-AVM; OMIM 608354) (Eerola, et al., 2003). CM-AVM is a familial vascular malformation syndrome that is also associated with high-flow arteriovenous malformations (AVM) or arteriovenous fistulas (AVF), or Parkes-Weber syndrome (PKWS; OMIM 608355) (Boon, Mulliken, & Vikkula, 2005; Frigerio, Stevenson, & Grimmer, 2012). *RASA1* is a p120-RasGAP that reverts active GTP-bound RAS to its inactive GDP-bound form to control cell differentiation and proliferation (Eerola, et al., 2003). Recently, Revencu et al. (2013) identified a somatic second-hit *RASA1* mutation in the dermal lesion of a CM-AVM patient.

The current treatment for PWS is pulsed dye laser (PDL) in combination with epidermal cooling, which lightens the vascular lesion in most cases (Kelly et al., 2005). However, there are a number of cases that respond very little, or not at all, to PDL treatment. Understanding the molecular background of PWS could potentially lead to more effective treatments.

This study was designed to investigate additional genetic variants and confirm the previously identified *GNAQ* c.548G>A, p.Arg183Gln in patients with isolated PWS. This

was done using a six gene custom capture next generation sequencing (NGS) panel that is able to detect low level mosaicism, ~0.1% (Wooderchak-Donahue et al., 2012). Digital polymerase chain reaction (dPCR) was used to confirm suspected variants identified by the custom NGS panel.

The majority of genes represented a variety of diseases that were either already associated with a CM or causative of other vascular malformations (Table 1). *GNAQ*, *RASA1*, and *SOX10* were included along with; *GLMN*, *TIE2/TEK*, and *PAX3*. *GLMN* and *TIE2/*TEK are both associated with venous malformations. Like *SOX10*, *PAX3* was investigated due to its role in neural crest development.

Table 1. Custom capture NGS genes

Gene Name	Chromosome Loci	Transcript ID	Gene Description	Disease	Exons
GNAQ	9q21	NM_002072	Guanine nucleotide binding protein	Decreased transcription, Increased promoter activity, Potential protein deficiency	7
RASA1	5q13.3	NM_002890	RAS p21 protein activator (GTPase activating protein) 1	Capillary malformations, Sturge-Weber syndrome, Parkes-Weber Syndrome,	25
SOX10	22q13.1	NM_006941	SRY (sex determining region Y) box 10	Waardenburg syndrome	4
PAX3	2q35	NM_181458	Paired box 3	Waardenburg syndrome	10
TIE2/TEK	9p21	NM_000459	TEK tyrosine kinase	Venous malformations	23
GLMN	7p22.1	NM_053274	Glomulin, FKBP associated protein	Glomulovenous malformations	19

MATERIALS AND METHODS

Sample Collection

Participants were recruited from adult patients who entered the Carolyn and Peter Lynch Laser Center at Massachusetts Eye and Ear Infirmary (MEEI) for treatment of their PWS. Individuals who met the following exclusion criteria were not included in the study: cognitively, visually, or hearing impaired persons; pregnant women; non-English speakers; individuals with associated venous or lymphatic malformations.

Eleven females and 1 male, ranging 18-72 years, were enrolled in the study. All PWS were isolated cases, i.e., not associated with any other vascular malformation. PWS were phenotyped using 3dMD photogrammetric software (3dMD; Atlanta, GA) according to a method previously described (Frigerio et al., 2014). Patient demographics and location of PWS are detailed in Table 2.

Two, 3 mm punch, skin samples were collected from each participant. One intra-lesional biopsy was performed on PWS skin and a second on apparently normal skin of the contralateral, corresponding body region. For each sample, a small part was formalin-fixed, paraffin embedded for histological staining. The remainder of the sample was flash frozen and stored at -80°C. Samples were shipped overnight on dry ice to ARUP Laboratories, University of Utah, Salt Lake City, UT, for DNA extraction and analysis. DNA from an unaffected female peripheral blood sample was used as a negative control.

Informed consent was obtained from each participant and the Declaration of

Table 2. Patient demographics and PWS location

Case #	Sex	Age (years)	PWS location	Side (R:right; L:left)
1	M	41	V2 dermatome	L
2	F	39	upper body	L
3	F	72	Wrist	R
4	F	29	V1 dermatome	L
5	F	18	V3 dermatome; C2 dermatome	R,L ; R
6	F	33	upper body	R,L
7	F	62	V2 dermatome; V3 dermatome	L ; R,L
8	F	28	half body	R,L
9	F	26	Shin	R
10	F	25	V1 dermatome	L
11	F	51	Forearm	L
12	F	45	V2 dermatome	R

Dermatome is an area of skin that is supplied by a single spinal nerve. V1,V2, V3 refers to the trigeminal nerve (fifth cranial nerve). C2 is the cervical vertebrae location.

Helsinki protocols were followed and written. Institutional review board approval was obtained by MEEI Human Studies Committee (IRB # 12-120H) and by the University of Utah Institutional Review Board (IRB # 00059017).

Tissue Sample Processing

DNA was extracted from 12 affected tissue samples and 12 unaffected tissue samples using the DNeasy Blood and Tissue Kit (Qiagen, Germantown, MD) protocol with a three day proteinase K incubation at 56° C. DNA concentrations were verified using a NanoDrop 8000 (Thermo Scientific, Wilmington, DE).

NGS Custom Capture

Custom capture RNA baits were designed to target the exons and exon/intron boundaries of the six genes in Table 1 (~0.04Mb). DNA from affected and control tissue (1.4-3µg) were sheared to 180 bp fragments using a Covaris instrument (Covaris, Woburn, MA). Illumina adapters were added using the SureSelect XT kit reagents (Agilent Technologies, Santa Clara, CA). Adapter ligated libraries were then hybridized with the biotinylated RNA baits at 65°C for 24 hours. Hybridized DNA targets of interest were captured using streptavidin coated magnetic beads. Targeted DNA were washed, eluted, and then barcoded/indexed. DNA quality was assessed using a Bioanalyzer (Agilent Technologies, Santa Clara, CA).

NGS Sequencing and Data Analysis

Concentrations of the indexed sample libraries were verified using quantitative PCR (KAPA Biosystems, Willmington, MA) and pooled together at a 1:1 ratio. Samples were sequenced on the HiSeq2500 instrument (Illumina, San Diego, CA) using 2x100 paired-end reads. Sequences were aligned to the human genome reference (GRCh37) sequence, using the Burrows-Wheeler Alignment tool (BWA 0.5.9) with default parameters. PCR duplicates were removed using the Samtools package, and base quality score recalibration was performed. Local realignment and variant calling were performed with the Genome Analysis Toolkit (GaTK v1.3). This method enables the detection of low level somatic insertions and deletions.

Low frequency (<10%) single nucleotide variants were detected using the subtractive correction method, as previously described (Margraf et al., 2010; Margraf et

al., 2011). Read coverage was gathered from the bam file data for each bed file position, as well as for the three possible nucleotide changes from the reference at each position. The reads were filtered out of the data set if < 25 mapping quality and either < 24 or <30 base quality (depended on average read coverage for each sample). For variant read frequencies presented in this paper, 24 base quality was used. For each position, the variant read frequency of the unaffected tissue was subtracted from the variant read frequency for the affected tissue. Variants were kept for further analysis if the variant read frequency percentage was at least 1% higher in the affected tissue versus the unaffected tissue.

Digital PCR (dPCR)

Digital PCR was used to confirm the presence of the following somatic mutations in the affected tissue samples: *GNAQ* p.Arg183Gln, *GNAQ* p.Arg183Gly, and *SOX10* p.Ala183Val. DNA from matched control tissues and one negative control sample from peripheral blood were also evaluated for each somatic mutation. A custom TaqMan SNP genotyping assay (Table 3) was optimized for each variant using the QuantStudio™ 3D Digital PCR System (Life Technologies, Grand Island, NY). Results were analyzed using the QuantStudio™ 3D AnalysisSuite™ software relative quantification module.

Table 3. Digital PCR TaqMan assay primer/probe sequences

	***GNAQ* p.Arg183Gln**	***GNAQ* p.Arg183Gly**	***SOX10* p.Ala183Val**
Forward Primer	CTGCCTACGCAACAAGATGTG	CTGCCTACGCAACAAGATGTG	CCCAGGCGGCGGAA
Reverse Primer	GGACTCAGTTACTACCTGAAAATGACA	GGACTCAGTTACTACCTGAAAATGACA	GTCCAAGTGGGCGCTCTT
Probe 1	TTAGAGTTCGAGTCCCC	CTTAGAGTTCGAGTCCC	TGGGCGGCCTTC
Probe 2	TTAGAGTTCAAGTCCCC	TTAGAGTTGGAGTCCC	TGGGCGACCTTC

RESULTS

Six genes, listed in Table 1, were used in the custom NGS panel to investigate the molecular characteristics of isolated PWS in 12 patients. For each case, a PWS affected tissue sample and a contralateral normal tissue sample were analyzed. DNA extracted from the peripheral blood from an unaffected female was used as a negative control. Examples of PWS are shown in Figure 1. Two Cases, 3 and 9, had no variants of interest identified in the custom NGS panel. Of the six genes in this panel, three of them had variants of interest in this cohort. The average NGS coverage for PWS tissue was 1,151 reads with a range of 447-2,595 reads. The coverage for control tissue ranged from 418-2,644 reads with an average of 1,936 reads. Variants of interest that were identified using the custom NGS panel were confirmed using dPCR. The dPCR method used has been shown to detect and quantify rare alleles with a frequency of 1% and higher (Life Technologies, Grand Island, NY).

GNAQ Variants Confirmed in Majority of Cases

The previously identified *GNAQ* p.Arg183Gln variant was identified in 9 of 12 cases (75%), as shown in Table 4. Figure 2 shows the *GNAQ* p.Arg183Gln NGS trace and dPCR results for Case 12. Variant allele frequencies from NGS ranged from 1.73% to 7.42% in the PWS affected tissue. Control tissue samples ranged from 0.00-0.13%, and DNA from the unaffected female was 0.06%. The dPCR data were highly concordant

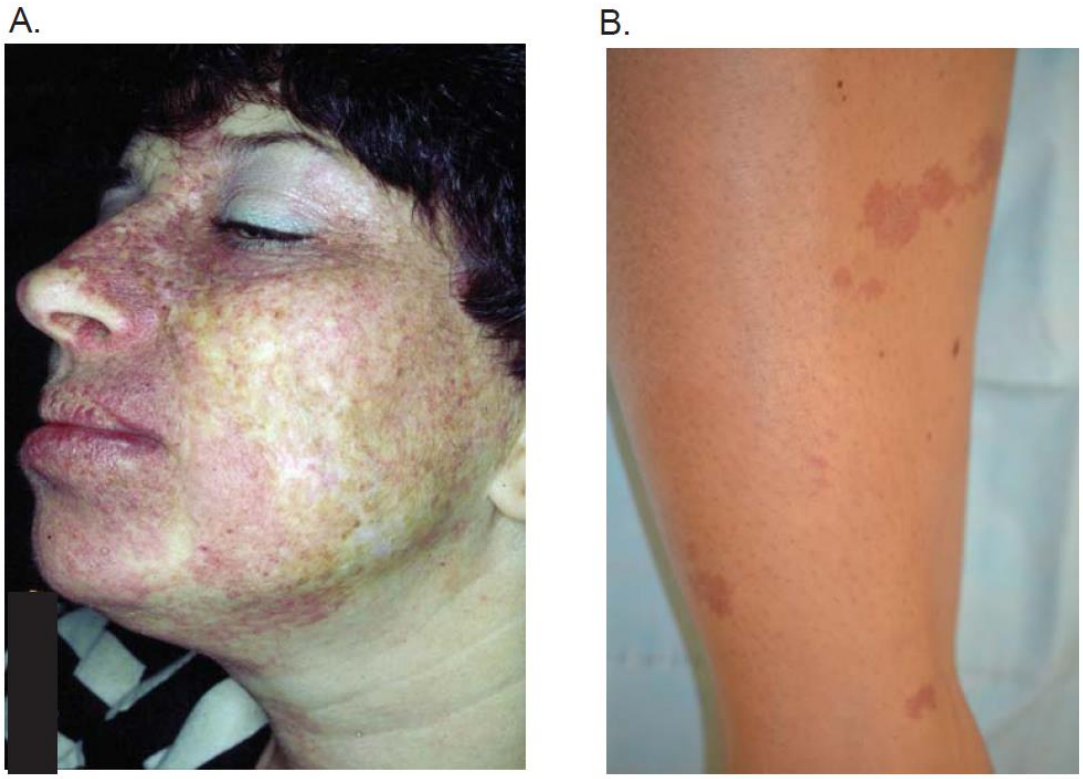

Figure 1.Case examples of port wine stains. (A) Case 7 harbors the novel *GNAQ* p.Arg183Gly variant. (B) PWS of Case 9 tested negative for the six panel genes.

with the NGS data. Digital PCR results had a range of 0.85% ± 0.04 to 7.42% ± 0.04 for PWS tissue; while the control tissue was 0.00% ± 0.01 to 0.80% ± 1.20. The unaffected female sample had a variant allele frequency of 0.22% ± 0.12.

A novel *GNAQ* variant p.Arg183Gly, c.547C>G was identified in Case 7 (Figure 3). The variant was detected in 4.05% of the NGS reads for the PWS tissue. Digital PCR assay confirmed the results at 3.76% ± 0.37 for PWS tissue. This is a highly conserved region and is predicted to be damaging by Mutation Taster, Polyphen, and SIFT (sorting intolerant from tolerant). Both the control tissue and unaffected female were negative for this variant.

Table 4. *GNAQ* p.Arg183Gln variant allele frequencies

		***GNAQ* p.Arg183Gln, c.548 G>A**		
Case		**Custom Capture (%)**	**dPCR (% ± SD)**	**Interpretation**
1	**PWS**	**2.66**	**4.86 ± 0.60**	**Positive**
	Ctrl	0.07	0.69 ± 0.97	
2	**PWS**	**5.80**	**6.35 ± 0.07**	**Positive**
	Ctrl	N/A	0.44 ± 0.10	
3	PWS	0.07	0.18 ± 0.15	Negative
	Ctrl	0.04	0.18 ± 0.01	
4	**PWS**	**1.76**	**1.61 ± 0.37**	**Positive**
	Ctrl	0.00	0.58 ± 0.41	
5	**PWS**	**3.31**	**5.44 ± 0.92**	**Positive**
	Ctrl	0.00	0.10 ± 0.04	
6	**PWS**	**3.98**	**3.69 ± 0.03**	**Positive**
	Ctrl	0.00	0.14 ± 0.01	
7	PWS	0.00	0.00	Novel *GNAQ*
	Ctrl	0.00	0.00	
8	**PWS**	**2.99**	**6.15 ± 0.44**	**Positive**
	Ctrl	N/A	0.49 ± 0.44	
9	PWS	0.13	0.11 ± 0.07	Negative
	Ctrl	N/A	0.00 ± 0.06	
10	**PWS**	**1.73**	**0.85 ± 0.04**	**Positive***
	Ctrl	N/A	0.28 ± 0.03	
11	**PWS**	**5.12**	**5.34 ± 0.20**	**Positive**
	Ctrl	N/A	0.80 ± 1.20	
12	**PWS**	**7.42**	**7.42 ± 0.04**	**Positive**
	Ctrl	0	0.63	
Unaffected Female		0.06	0.22 ± 0.12	Negative

* dPCR detection limit is 1%. However, this case was interpreted as positive by combining NGS data and dPCR value (close to 1%).

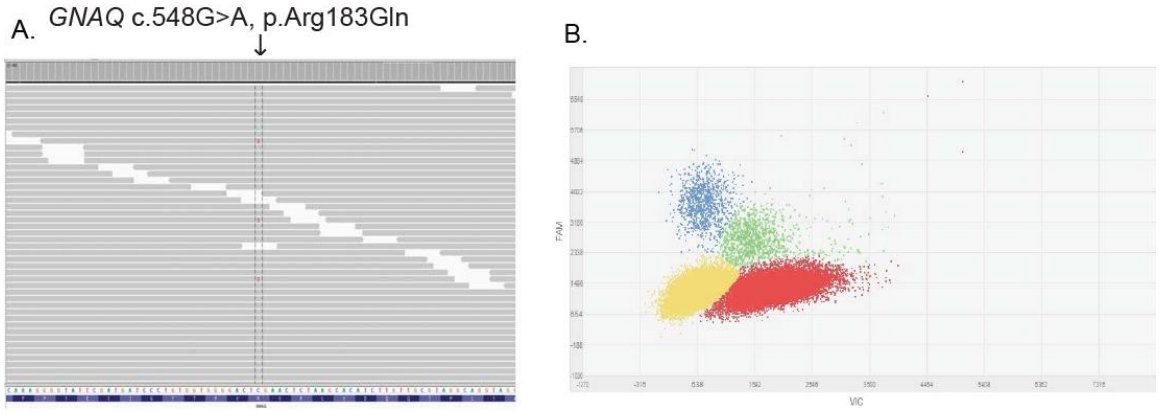

Figure 2. Case 12 *GNAQ* p.Arg183Gln NGS trace and dPCR amplification plot. (A) NGS trace for Case 12 showing the complement strand C>T base change. (B) dPCR results of Case 12. Variant alleles represented by blue, wild type alleles represented by red. Green is both variant and wild type alleles. Yellow is no amplification.

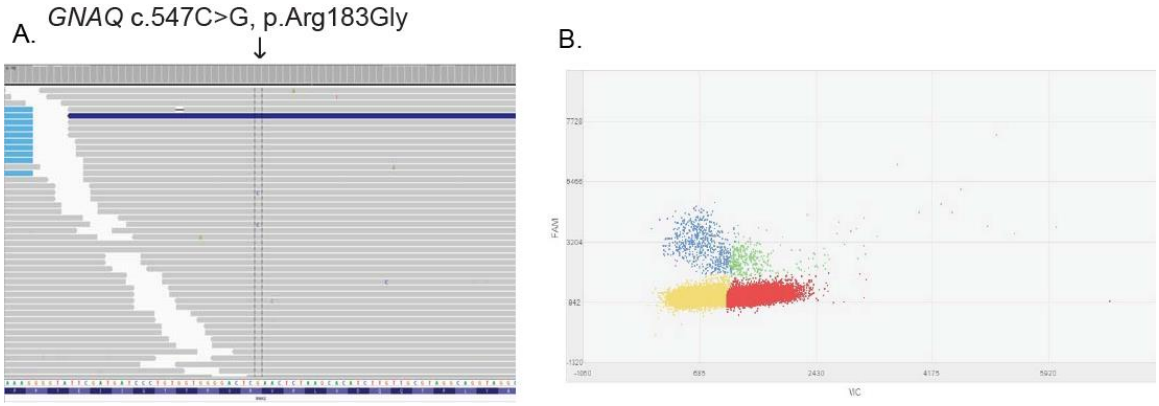

Figure 3. Case 7 *GNAQ* p.Arg183Gly NGS trace and dPCR amplification plot. (A) NGS trace showing the complement strand G>C base change. (B) dPCR results of Case 7. Variant alleles represented by blue, wild type alleles represented by red. Green is both variant and wild type alleles. Yellow is no amplification.

Novel Variant Identified in *SOX10*

A novel variant, *SOX10* p.Ala183Val c.548C>T, was identified in Case 8 with an allele frequency of 0.93% from the NGS data (Figure 4). A control tissue sample for this case was not available for NGS, but the wild type female had an allele frequency of 0.16%. Many attempts were made to optimize the dPCR assay for this variant. However, due to the high GC content in this region, the assay failed to perform. This variant was not in publicly available domains such as Exome Variant Server, Exome Aggregation Consortium, or COSMIC. The potential effects of this variant were identified in Mutation Taster and PolyPhen as disease causing, but SIFT predicted the variant would be tolerated.

Interesting *RASA1* Variants

Two different *RASA1* variants were identified in this cohort. Case 5 had a novel variant, *RASA1* p.Arg579Arg c.1735C>A, identified in 1.80% of the NGS reads (Figure 5a). Case 7 had a variant upstream from the 5'UTR region, c.-222G>A, of 1.90% in the PWS tissue (Figure 5b). In both cases, the control tissue and wild type female were negative for these variants. Confirmation with dPCR was not done on either variant owing to the prediction that they would not affect splicing, or translation or transcription factor binding (Desmet et al., 2009).

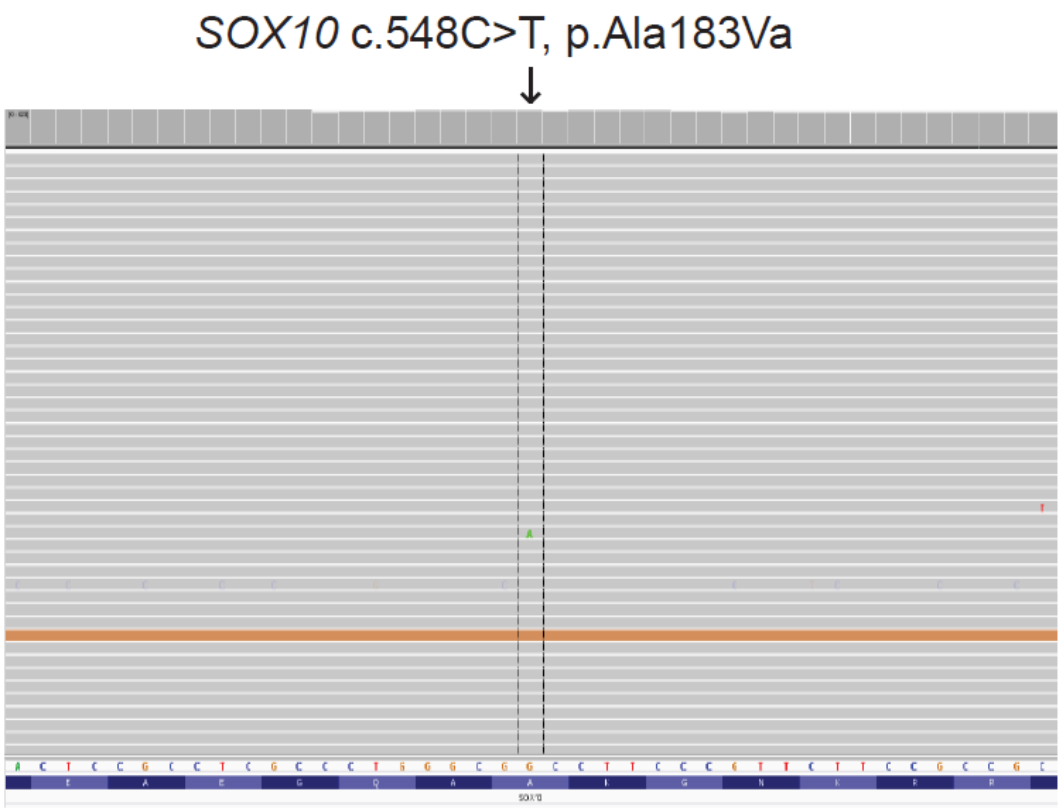

Figure 4. Case 8 *SOX10* p.Ala183Val NGS trace. The complement strand for Case 8 showing the G>A base change.

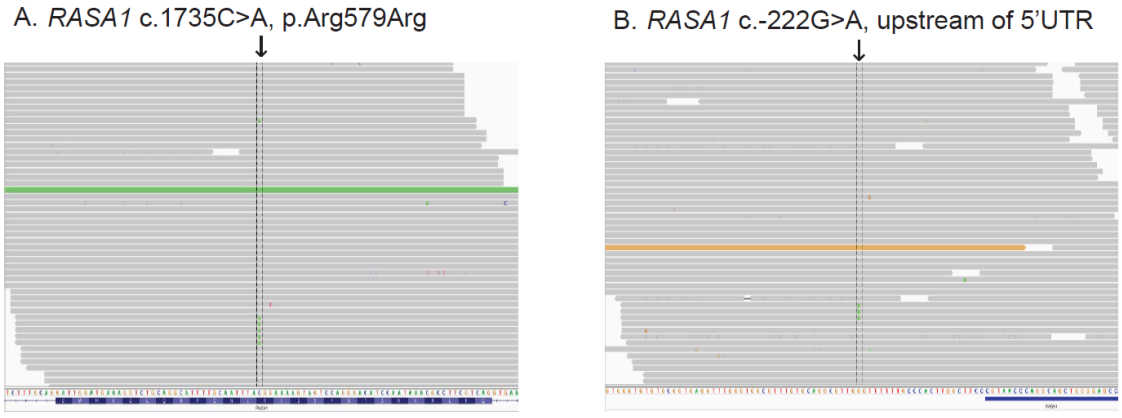

Figure 5. *RASA1* variants of interest NGS traces. (A) NGS trace for Case 5 showing the C>A base change. (B) NGS trace of Case 7 showing the 5'UTR G>A base change.

DISCUSSION

Most cases of PWS occur as sporadic, isolated dermatomal lesions. Smoller and Rosen (1986) have proposed that lack of innervation leads to PWS. Sanchez-Carpintero et al. (2004) noted complex hamartomatous changes in the PWS involved multiple germ lines, which suggests multilineage developmental field defects might be responsible for the pathogenesis of PWS. In this study six genes (Table 1) were investigated for variants of interest in a cohort of isolated PWS cases.

GNAQ was included to confirm the presence of a previously identified variant and other possible variants in this cohort of isolated PWS. Shirley et al. (2013) demonstrated that p.Arg183Gln c.548G>A was a somatic activating mutation in 92% of isolated PWS samples and 88% of patients with Sturge-Weber syndrome. The variant allele frequencies reported by Shirley et al. (2013) ranged from 1.0-18.1%, while this cohort ranged from 0.85-7.42%. The difference in allele frequencies can be explained by the different procedures. This study used a subtractive correction method that eliminated much of the background noise in the NGS data (Margraf et al., 2010; Margraf et al., 2011). Using dPCR (~1% limit of detection) as a confirmatory assay provided a more accurate data set at such low levels of mosaicism.

The novel *GNAQ* variant (p.Arg183Gly, c.547C>G) detected in the PWS skin of Case 7 is located in the same amino acid residue as the variant identified by Shirley et al. (2013), p.Arg183Gln, c.548G>A. This particular amino acid residue, arginine, is critical

to the function of the GTP binding pocket of all human Gα subunits. The positive charge of arginine stabilizes the negative charge of the penta-coordinate phosphate intermediate, facilitating hydrolysis of the phosphate group and inactivates the protein (Coleman et al., 1994). Substitution of this residue to either a polar glutamine or hydrophobic glycine residue, likely impairs hydrolysis, such that GNAQ remains in its active GTP-bound form, resulting in the observed PWS phenotype. The novel p.Arg183Gly variant has not been previously reported in any databases and was predicted to be damaging by multiple prediction algorithms.

Among the cases positive for *GNAQ* mutations, there was no correlation between anatomical site and the mutation level. Two Cases, 3 and 9, have PWS of the limbs and had no variants of interest in any of the six genes used in this NGS panel. Case 11 has a PWS of the forearm and is positive for the *GNAQ* variant. There are phenotypic differences, as shown in Figure 1, between the positive and negative cases which may impact the variant frequency. Further studies will need to confirm this theory.

Recently, Lian et al. (2014) identified additional novel somatic mutations in *SMARCA4, EPHA3, MYB, PDGFR-β,* and *PIK3CA* in an isolated PWS using exome sequencing. These genes are involved in angiogenesis, embryonic venous specification, and proliferation of vascular smooth muscle cells (Lian et al., 2014). Adding these genes to future NGS panels could help identify the genetic determinates of those cases with no *GNAQ* somatic variants.

At the molecular level, significant ERK (extracellular signal-regulated kinases) activation has been observed in human embryonic kidney cells transfected with *GNAQ* p.Arg183Gln, as compared with cells transfected with nonmutant GNAQ (Shirley et al.,

2013). The mutation did not seem to activate other MAPK (mitogen-activated protein kinase) pathway members or the AKT (protein kinase B) signaling pathway. It is likely that the novel *GNAQ* p.Arg183Gly variant is also an activating mutation because it disrupts the same critical arginine residue. More recent data report the activation of ERK and JNK (c-Jun N-terminal kinase) in 19 of 19 PWS samples. JNK activation levels appeared correlated to the progressive development of PWS (Tan et al., 2014). *GNAQ's* gain-of-function properties and how they influence the PWS phenotype will require further research to understand this delicate balance.

This study also identified two novel somatic *RASA1* variants (Figure 4). In these Cases (5 and 7), PWS involve cervicofacial dermatomes and also harbor *GNAQ* somatic variants, one of which (Case 7) has the novel p.Arg183Gly (Figure 2). No additional *RASA1* germline mutations were found in these 2 participants. Currently, *RASA1* changes are not seen as main genetic determinants in the pathogenesis of the studied PWS. Interestingly, a recent study reported that *RASA1* does not seem to be involved as a genetic determinant of most familial PWS (Rubin et al., 2015).

A mosaic missense mutation of *SOX10* (p.Ala183Val, c.548C >T) was found in Case 8 (Figure 3). This patient is a woman affected by a massive PWS which involves more than a half of her body surface. This phenotype could be explained by an early disruption of the dermal vascular development. It is unclear whether a somatic mutation of *SOX10* may have played a role in the fate specification of migrating neural crest cells at an early stage of development in this case.

Of the three genes that no variants of interest were identified in, *GLMN* and *TIE2/TEK* have been identified in other vascular anomalies. *GLMN* variants are seen in

familial cases of glomulovenous malformations (Brouillard et al., 2013). *TIE2/TEK* is also associated with venous malformations and has been shown to be critical to the survival of vascular endothelial cells (Vikkula et al., 1996). *PAX3* was investigated, along with *SOX10*, because of its role during neural crest development and the hypothesis that PWS could originate from neural crest cells due to their facial location. *PAX3* has been shown to initiate neural crest specification and trigger full neural crest determination in Xenopus embryos (Milet, Maczkowiak, Roche, & Monsoro-Burg, 2013).

CONCLUSION

This study corroborates the hypothesis that *GNAQ* mutation represents one of the most important PWS pathogenic factors in the early stages of development and that other genetic factors may also be involved in the pathogenesis of PWS. Future directions for this project will be to analyze the exome data for all 12 cases using the same subtractive corrective method to identify additional molecular characteristics of PWS. New PWS cases will be analyzed using the same methods when they become available. In addition to that, further studies are needed to identify the cell types these mutations are happening in. This could likely increase the ability to see such low frequency variations if DNA was from the appropriate cell type instead of a mixed cell population.

REFERENCES

Bondurand N., Pingault V., Goerich D.E., Lemort N., Sock E., Le Caignec C., … Goossens M. (2000). Interaction among SOX10, PAX3, and MITF, three genes altered in Waardenburg syndrome. *Human Molecular Genetics, 9*, 1907-1917.

Boon L.M., Mulliken J.B., & Vikkula M. (2005). RASA1: Variable phenotype with capillary and arteriovenous malformations. *Current Opinion in Genetics & Development, 15*, 265-269.

Brouillard P., Boon L.M., Revencu N., Berg J., Dompmartin A., Dubois J., … GVM Study Group. (2013). Genotypes and phenotypes of 162 families with a glomulin mutation. *Molecular Syndromology, 4*, 157-164.

Coleman D. E., Berghuis A.M., Lee E., Linder M.E., Gilman A.G., & Sprang S.R. (1994). Structures of active conformations of Gi alpha 1 and the mechanism of GTP hydrolysis. *Science, 265*, 1405-1412.

Desmet F.O., Hamroun D., Lalande M., Collod-Béroud G., Claustres M., & Béroud C. (2009). Human splicing finder: An online bioinformatics tool to predict splicing signals. *Nucleic Acids Research, 37*, 67.

Eerola I., Boon L.M., Mulliken J.B., Burrows P.E., Dompmartin A., Watanabe S., … Vikkula M. (2003). Capillary malformation-arteriovenous malformation, a new clinical and genetic disorder caused by RASA1 mutations. *American Journal of Human Genetics, 73*, 1240-1249.

Frigerio A., Bhama P.K., & Tan O.T. (2014). Quantitative three-dimensional assessment of port wine stain clearance after laser treatments. *Lasers in Surgery and Medicine, 46*, 180-185.

Frigerio A., Stevenson D.A., & Grimmer J.F. (2012). The genetics of vascular anomalies. *Current Opinion in Otolaryngology & Head and Neck Surgery, 20*, 527-532.

Happle R. (1987). Lethal genes surviving by mosaicism: A possible explanation for sporadic birth defects involving the skin. *Journal of the American Academy of Dermatology, 16*, 899-906.

Jacobs A.H. & Walton R.G. (1976). The incidence of birthmarks in the neonate. *Pediatrics, 58*, 218-222.

Kelly K.M., Choi B., McFarlane S., Motosue A., Jung B., Khan M.H. … Nelson J.S. (2005). Description and analysis of treatments for port wine stain birthmarks. *Archives of Facial Plastic Surgery, 7*, 287-294.

Lian C.G., Sholl L.M., Zakka L.R., O T.M., Liu C., Xu S., … Mihm M.C. Jr. (2014). Novel genetic mutations in a sporadic port wine stain. *JAMA Dermatology, 150*, 1336-1340.

Lowe L.H., Marchant T.C., Rivard D.C., & Scherbel A.J. (2012). Vascular anomalies: Classification and terminology the radiologist needs to know. *Seminars in Roentgenology, 47*, 106-117.

Margraf R.L, Durtschi J.D., Dames S., Pattison D.C., Stephens J.E., Mao R., & Voelkerding K.V. (2010). Multi-sample pooling and Illumina genome analyzer sequencing methods to determine gene sequence variation for database development. *Journal of Biomolecular Techniques, 21*, 126-140.

Margraf R.L, Durtschi J.D., Dames S., Pattison D.C., Stephens J.E., & Voelkerding K.V. (2011). Variant identification in multi-sample pools by Illumina genome analyzer sequencing. *Journal of Biomolecular Techniques, 22*, 74-84.

Milet C., Maczkowiak F., Roche D.D., & Monsoro-Burg A.H. (2013). Pax3 and Zic1 drive induction and differentiation of multipotent, migratory, and functional neural crest in Xenopus embryos. *Proceedings of the National Academy of Sciences of the United States of America, 110*, 5528-5533.

Revencu N., Boon L.M., Mendola A., Cordisco M.R., Dubois J., Clapuyt P., …Vikkula M. (2013). RASA1 mutations and associated phenotypes in 68 families with capillary malformation-arteriovenous malformation. *Human Mutation, 34*, 1632-1641.

Rubin A., Lauritzen E., Ljunggren B., Revencu N.,Vikkula M., & Svensson A. (2015). The heredity of port wine stains: Investigation of families without a RASA1 mutation. *Journal of Cosmetic and Laser Therapy: Official Publication of the European Society for Laser Dermatology, 20*, 1-13.

Sanchez-Carpintero I., Mihm M.C., Mizeracki A., Waner M., & North P.E. (2004). Epithelial and mesenchymal hamartomatous changes in a mature port wine stain: Morphologic evidence for a multiple germ layer field defect. *Journal of the American Academy of Dermatology, 50*, 608-612.

Shirley M.D., Tang H., Gallione C.J., Baugher J.D., Frelin L.P., Cohen B., … Pevsner J. (2013). Sturge-Weber syndrome and port wine stains caused by somatic mutation in GNAQ. *The New England Journal of Medicine, 368*, 1971-1979.

Smoller B.R. & Rosen S. (1986) Port wine stains. A disease of altered neural modulation of blood vessels? *Archives of Dermatology, 122,* 177-9.

Tan W., Chernova M., Gao L., Sun V., Liu H., Jia W., … Nelson J.S. (2014). Sustained activation of c-Jun N-terminal and extracellular signal-regulated kinases in port wine stain blood vessels. *Journal of the American Academy of Dermatology, 71*, 964-968.

Vikkula M., Boon L.M., Carraway K.L. 3rd, Calvert J.T., Diamonti A.J., Goumnerov B., … Olsen B.R. (1996). Vascular dysmorphogenesis caused by an activating mutation in the receptor tyrosine kinase TIE2. *Cell, 87*, 1181-1190.

Wooderchak-Donahue W.L., O'Fallon B., Furtado L.V., Durtschi J.D., Plant P., Ridge P.G., … Bayrak-Toydemir P. (2012). A direct comparison of next generation sequencing enrichment methods using an aortopathy gene panel-clinical diagnostics perspective. *BMC Medical Genomics, 14*, 50.